35th Annual International Conference of the IEEE EMBS
Osaka, Japan, 3 - 7 July, 2013

Denoising 3D Ultrasound Volumes Using Sparse Representation

Dae Hoe Kim[1], Konstantinos N. Plataniotis[2], and Yong Man Ro[1]

Abstract— **In this paper, a new 3D ultrasound (US) denoising technique that adopts the sparse representation has been proposed for an effective noise reduction in 3D US volumes. The purpose of the proposed method is to reduce image noise while preserving 3D objects edges, hence improving the human interpretation for clinical diagnosis and the 3D segmentation accuracy for further automatic malignancy detection. For denoising 3D US volumes, sparse representation was employed, which has showed an excellent performance in reducing Gaussian noise. It has been well known that US images contain severe multiplicative speckle noise, which has different characteristics compared to the additive Gaussian noise. In this paper, we propose a denoising framework for effectively reducing both Gaussian noise and speckle noise on 3D US volumes. The proposed method removes Gaussian noise using sparse representation. Then, a logarithmic transform is performed to transform the speckle noise into Gaussian noise for applying the sparse representation. To demonstrate the effectiveness of the proposed denoising method, comparative and quantitative experiments had been conducted on a synthesized 3D US phantom data. Experimental results showed that the proposed denoising could improve image quality in terms of denoising measurements.**

I. Introduction

Ultrasound (US) imaging has been widely used in clinical diagnosis because it is a non-invasive, non-radioactive, portable, real-time and low-cost imaging modality [1]. Most of current US imaging systems use 2D imaging methods. However, in conventional 2D US imaging it is difficult to reproduce the same image plane for follow-up studies, therefore the volume of an object is calculated approximately. In many cases, volume measurement is important in assessing the progression of disease and/or tracking progression of response to a treatment. Thus, 3D US imaging has drawn much attention to overcome this problem [2].

Although there are many advantages on US imaging, they contain a large amount of speckle noise that degrades both the spatial resolution and contrast quality in ultrasound images [3]. This speckle noise makes the interpretation or the mass segmentation of ultrasound images more difficult. Especially, reduced segmentation accuracy degrades automatic malignancy detection processes such as the feature extraction and classification of the malignancy. Therefore, in US imaging, an effective denoising is an essential preprocessing for improving the human interpretation, accurate segmentation.

Considerable research efforts have been made to develop denoising algorithms that effectively reduce image noise while preserving edge information. Yu *et al*. [4] proposed a speckle reducing anisotropic diffusion (SRAD) that combines conventional anisotropic diffusion filter and speckle reducing filter. The method diffuses intensities based on the gradient magnitude (edge) and the speckle noise level. Tay *et al*. [5] proposed a squeeze box filter (SBF) which suppresses outliers (local extrema) as a local mean of its neighborhood. In [5], experimental results showed that the SBF improves the image quality in terms of denoising measurements. Though aforementioned methods showed effective denoising results, some artifacts like an edge blur or an irregular intensity pattern on edges were occurred. In 3D US images, the best denoising algorithm for effectively preserving objects edges with fewer artifacts is still in question.

In this paper, we propose a new 3D US denoising algorithm that is based on sparse representation, aiming to effectively reduce image noise while preserving 3D edge information with the fewest artifacts. The basic concept of the sparse representation is that natural signals can be efficiently represented as a linear combination of atoms, where the linear coefficients are represented in a sparse domain. In [6], the sparse representation showed a significant performance in the additive Gaussian noise reduction. However, US volumes have severe multiplicative speckle noises [3]. Therefore, the proposed method adopts logarithmic transform to convert the multiplicative speckle noise into an additive Gaussian noise [7]. In the proposed denoising method, Gaussian noises are reduced by the sparse representation. Then, speckle noise is transformed into Gaussian noise by applying a logarithmic transform. Lastly, the sparse representation based denoising is performed on the Gaussianized speckle noise. To the best of our knowledge, our work is the first attempt to adopt sparse representation in the field of 3D US volume denoising. Using a synthesized 3D US phantom data, comparative and extensive experiments have been carried out. Experimental results show that the proposed sparse representation based 3D US denoising outperformed other denoising methods in terms of denoising measurements.

The rest of the paper is organized as follows. In section II, the sparse representation on 3D US volume is explained. Section III details the proposed 3D US denoising method. In section IV, experimental results are presented. The conclusion is drawn in section V.

II. Sparse Representation of 3D US Images

Recently, sparse representation (SR) [6, 8, 9] has been a popular research topic in the signal processing society. The fundamental sparse representation of 3D US image is that US image voxels can be efficiently approximated as a linear combination of 3D atoms, where the linear coefficients are represented in a sparse domain [6]. This process is referred to as sparse coding. In the sparse representation, the 3D US image can be approximated as follows:

[1]Image and Video Systems Laboratory, Korea Advanced Institute of Science and Technology (KAIST), Yuseong-Gu, Daejeon, 305-701, Korea, [2]The Edward S Rogers Sr Department of Electrical and Computer Engineering, University of Toronto, Toronto, Ontario, M5S 3GA, Canada

$$\hat{\boldsymbol{\alpha}} = \arg\min \|\boldsymbol{\alpha}\|_0^0 \text{ subject to } \|\mathbf{D}\boldsymbol{\alpha} - \mathbf{y}\|_2 \le \sigma\varepsilon', \quad (1)$$

where $\hat{\boldsymbol{\alpha}}$ is the sparse representation (sparse coefficient) of the noisy input 3D US volume patch $\mathbf{y}$, ε' is the error tolerance used to determine the target error for sparse-coding each block, σ is the noise standard deviation, the function $\|\cdot\|_0^0$ is $l^0 norm$, and $\mathbf{D}$ is the dictionary.

Equation (1) assumes the noisy 3D US volume $\mathbf{y}$ can be sparsely represented as $\mathbf{y} \approx \mathbf{D}\boldsymbol{\alpha}$. Based on that assumption, the sparse representation minimizes the difference of noisy patch and denoised patch, at the same time, minimizes $l^0 norm$ of $\boldsymbol{\alpha}$. To solve the above equation, we use batch orthogonal matching pursuit (OMP) [10] which is faster version of OMP.

The fundamental consideration of the above approximation is the choice of the dictionary $\mathbf{D}$. The dictionary can be either chosen as a pre-specified transform matrix (*e.g.* overcomplete discrete cosine transform (DCT) [11]), or be learnt by adapting its content to the given set of signal examples (*e.g.* K-singular value decomposition (SVD) [12]). The first approach is simple and straightforward, while the second approach shows a better approximation due to its adaptive property. The first approach is much less computationally demanding while the K-SVD approach provides a better sparsity level resulting in an improved representation with the same number of coefficient with a DCT dictionary. To take the complementary effect of both approaches, dictionary learning method using sparse K-SVD is employed [6]. The essential idea is that the dictionary $\mathbf{D}$ itself has a sparse representation over some pre-specified base dictionary $\boldsymbol{\Phi}$ as follows:

$$\mathbf{D} = \boldsymbol{\Phi}\mathbf{A}, \quad (2)$$

where $\mathbf{A}$ is the atom representation matrix.

III. Proposed Denoising 3D US Volumes Using Sparse Representation

The sparse representation based denoising is known to be effective for suppressing Gaussian noise in CT volumes [6]. However, US volumes have severe multiplicative speckle noise. The speckle noise model can be represented as in [5],

$$\mathbf{Y} = \eta_s \times \mathbf{X} + \eta_g, \quad (3)$$

where $\mathbf{X}$ is the noise free volume, $\mathbf{Y}$ is the noisy volume, η_s is the multiplicative speckle noise and η_g is the additive Gaussian noise.

We develop a sparse representation based denoising framework for reducing speckle noises as shown in Fig. 1. The proposed denoising method has two steps; the first is additive noise reduction and the second is multiplicative noise reduction. The first additive noise reduction is performed by solving following optimization problem using maximum a posteriori (MAP) [8]:

$$\left\{\hat{\mathbf{D}}, \hat{\mathbf{a}}_i, \hat{\mathbf{X}}\right\} = \arg\min_{\mathbf{D},\hat{\mathbf{a}}_i,\mathbf{X}} \lambda\|\mathbf{X} - \mathbf{Y}\|_2^2 + \sum_i \mu_i \|\mathbf{a}_i\|_0 + \sum_i \|\mathbf{D}\mathbf{a}_i - \mathbf{R}_i\mathbf{X}\|_2^2, \quad (4)$$

where λ is a Lagrange multiplier, $\mathbf{a}_i$ is the sparse vector of *i*-th volume patch, $\mathbf{R}_i$ is an operator that extracts *i-th* volume patches of $\mathbf{X}$, and $\hat{\mathbf{X}}$ is the denoised volume.

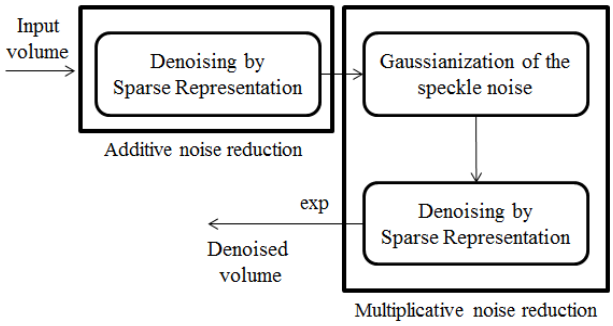

Figure 1. Block diagram of the developed 3D US denoising using sparse representation.

By solving (4) with (3), Gaussian noise is suppressed to get the volume $\hat{\mathbf{X}}_s$ that contains speckle noise only,

$$\hat{\mathbf{X}}_s = \eta_s \times \mathbf{X}. \quad (5)$$

Note that, generally, it is known the effect of additive noise is considerably small compared to that of multiplicative noise [13, 14]. Thus, the residual of additive noise can be ignored.

It has been known that speckle noise can be transformed into a Gaussian noise by the logarithmic operator [7]. For an effective speckle noise reduction in the second step in Fig.1, the logarithmic function is applied to the volume $\hat{\mathbf{X}}_s$,

$$\ln \hat{\mathbf{X}}_s = \ln \mathbf{X} + \ln \eta_s. \quad (6)$$

Then, the Gaussianized speckle noise is suppressed by using same sparse representation model like (4),

$$\ln \hat{\mathbf{X}} \approx \ln \mathbf{X}. \quad (7)$$

The final denoised volume can be attained by taking the exponential operation on (7).

IV. Experiments

A. Experimental condition

In experiments, denoising performance of the proposed method was evaluated. It is hard to compare denoising algorithms quantitatively in real US volumes because noise free US volume is not available in practice. In this paper, we generated a synthetic 3D US phantom (see Fig. 2) using the method of [4, 15, 16] for quantitative performance evaluations. The size of the phantom was 256 x 256 x 128 voxels in *x*, *y* and *z* directions, respectively. The volume contained three spheres with different radius. The phantom was simulated with following imaging parameter settings: center frequency was 10MHz, pulse-width and beam-width of transmitting US wave was 2 and 1.5 respectively as in [4]. For the comparisons of the proposed method to existing denoising methods, 3D version of SRAD and SBF were implemented and evaluated. To perform extensive comparisons, a grid search was performed varying the parameters of each denoising method so that the corresponding denoising performance measurement was maximized as in [5].

B. Denoising performance measurement

Four performance metrics were employed in the experiments to measure the denoising performances. Those are:

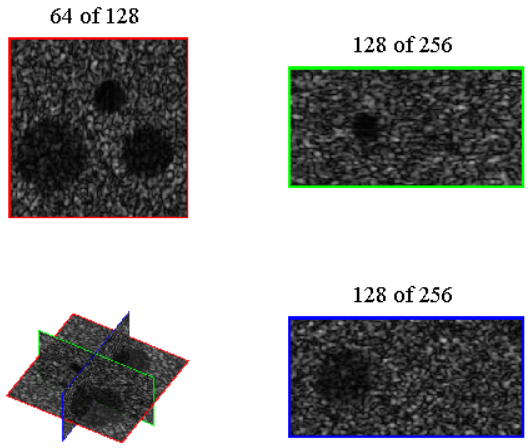

Figure 2. The synthesized 3D US phantom used in the experiment. The lower left 3D view shows how 2D slices are oriented in the volume. Three slice views show 2D slices of the volume along three different planes (red, green, and blue planes). The numbers above slice views show the index of the slice per total slices (*e.g.* 128) in those directions in the volume.

1) *US despeckling assessment index* (*USDSAI*) [5]

We measure the degree of preserved homogeneous region and of object separation. It can be written as,

$$Q(\hat{\mathbf{X}}) = \frac{\sum_{k \neq l} (\mu_{C_k} - \mu_{C_l})^2}{(N-1)\sum_{k=1}^{N} \sigma_{C_k}^2}, \quad (8)$$

where μ_{C_k}, $\sigma_{C_k}^2$ are mean and variance of voxel intensities of the region C_k in the denoised volume $\hat{\mathbf{X}}$.

To avoid sensitivity to resolution, the USDSAI is normalized regarding to the noisy volume $\mathbf{Y}$ as,

$$\hat{Q}(\hat{\mathbf{X}}) = Q(\hat{\mathbf{X}}) / Q(\mathbf{Y}). \quad (9)$$

The USDSAI is increased when objects are well distinct and homogeneous.

2) *Mean structural similarity* (*MSSIM*) [17]

We measure the local structural-similarity of a volume against a noise free volume (the ground truth). It is measured as the mean of each voxel's SSIM values. The SSIM is derived as,

$$SSIM = \frac{(2\mu_x\mu_y + c_1)(2\sigma_{xy} + c_2)}{(\mu_x^2 + \mu_y^2 + c_1)(\sigma_x^2 + \sigma_y^2 + c_2)}, \quad (10)$$

where x, y are two 8x8x8 cropped local volumes from a ground truth and a denoised volume. $c_1 = (k_1 L)^2$, $c_2 = (k_2 L)^2$ which to stabilize the division with weak denominator. L is the dynamic range of the pixel-values. k_1=0.01 and k_2=0.03 as default values.

The SSIM index varies between -1 to 1, where 1 indicates the best local similarity to the ground truth.

3) *Edge preservation index* (*EPI*) [18]

We measure edge strength correlations as EPI:

$$\alpha = \frac{\Gamma(\Delta\mathbf{X} - \overline{\Delta\mathbf{X}}, \Delta\hat{\mathbf{X}} - \overline{\Delta\hat{\mathbf{X}}})}{\sqrt{\Gamma(\Delta\mathbf{X} - \overline{\Delta\mathbf{X}}, \Delta\mathbf{X} - \overline{\Delta\mathbf{X}}) \cdot \Gamma(\Delta\hat{\mathbf{X}} - \overline{\Delta\hat{\mathbf{X}}}, \Delta\hat{\mathbf{X}} - \overline{\Delta\hat{\mathbf{X}}})}}, \quad (11)$$

$$\Gamma(\mathbf{X}_1, \mathbf{X}_2) = \sum_{(x,y,z) \in VOI} \mathbf{X}_1(x,y,z) \cdot \mathbf{X}_2(x,y,z), \quad (12)$$

where $\Delta\mathbf{X}$ and $\Delta\hat{\mathbf{X}}$ are high pass filtered versions of $\mathbf{X}$ and $\hat{\mathbf{X}}$, obtained with a 3 x 3 Laplacian operator.

The edge preservation index is increased when the denoised volume is similar to the ground truth.

4) *Noise suppression index* (*NSI*) [18]

We measure voxel intensity correlation as NSI:

$$\beta = \frac{\Gamma(\mathbf{X} - \overline{\mathbf{X}}, \hat{\mathbf{X}} - \overline{\hat{\mathbf{X}}})}{\sqrt{\Gamma(\mathbf{X} - \overline{\mathbf{X}}, \mathbf{X} - \overline{\mathbf{X}}) \cdot \Gamma(\hat{\mathbf{X}} - \overline{\hat{\mathbf{X}}}, \hat{\mathbf{X}} - \overline{\hat{\mathbf{X}}})}}, \quad (13)$$

where $\overline{\mathbf{X}}$ and $\overline{\hat{\mathbf{X}}}$ are the mean intensity values of the VOI of $\mathbf{X}$ and $\hat{\mathbf{X}}$.

The noise suppression index is increased when the denoised volume is similar to the ground truth.

C. Experimental results

Table I shows the measured denoising performances for the denoising algorithms on the 3D US phantom. The first column in Table I shows the performance metric in which the algorithms are optimized. The bold numeric shows the best performance among three methods (SRAD, SBF, proposed) with respect to the corresponding performance metric. As shown in the results of the Table I, the proposed denoising outperforms other two methods in terms of denoising performance metrics, especially USDSAI and edge preservation index for every optimization criteria. The denoised volume using the proposed denoising method had more differentiable objects (higher USDSAI), and preserved more clear edges. Fig. 3 shows denoised phantoms for the denoising algorithms, which were optimized based on the metric of USDSAI. As shown in the figures, the proposed denoising method effectively reduces image noise while preserving the edges.

TABLE I. COMPARISONS OF MEASURED DENOISING PERFORMANCES

Optimization criteria	Measured performance	Denoising algorithm		
		SRAD	SBF	Proposed
USDSAI	USDSAI	4.1443	4.4702	**6.2346**
	MSSIM	**0.4487**	0.4229	0.4048
	EPI	0.0036	0.0007	**0.0071**
	NSI	**0.8266**	0.6759	0.7996
MSSIM	USDSAI	3.9454	4.4702	**5.3820**
	MSSIM	**0.4642**	0.4229	0.4482
	EPI	0.0023	0.0007	**0.0040**
	NSI	**0.8754**	0.6759	0.8639
EPI	USDSAI	3.3456	4.1230	**5.7691**
	MSSIM	0.3521	**0.4162**	0.3985
	EPI	0.0078	0.0008	**0.0136**
	NSI	0.6530	0.6765	**0.7750**
NSI	USDSAI	3.9454	4.2816	**4.5825**
	MSSIM	**0.4642**	0.4198	0.4481
	EPI	0.0023	0.0007	**0.0052**
	NSI	**0.8754**	0.6771	0.8642

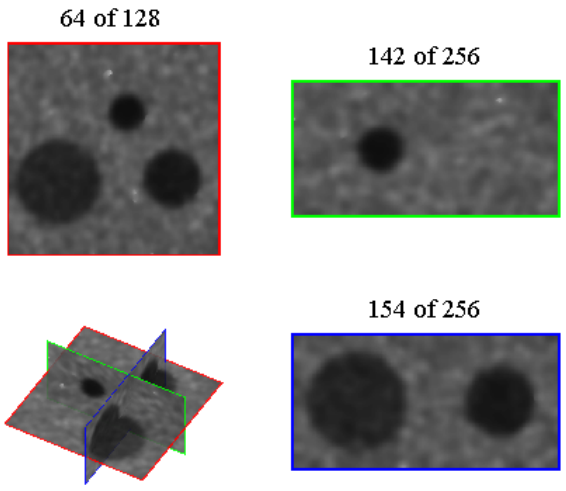

Figure 3. Denoised results on 3D US phantom using (a) SRAD, (b) SBF, (c) proposed sparse representation based denoising method. Note edge blur and irregular intensity pattern on edges were found in SRAD and SBF, respectively.

V. Conclusion

In this paper, we proposed a new 3D US volume denoising technique to reduce image noise while preserving 3D objects edges. We employed sparse representation of 3D US volume, which showed an excellent performance in reducing Gaussian noise. We developed a denoising framework for effectively reducing both Gaussian noise and speckle noise on 3D US volumes. To demonstrate the effectiveness of the proposed denoising method, comparative and quantitative experiments had been conducted on a synthesized 3D US phantom data. In experiments, the proposed denoising outperforms existing two methods in terms of denoising performance metrics. The denoised volume by the proposed method showed more differentiable objects and preserved more clear edges.

References

[1] F. W. Kremkau and G. Gooding, *Diagnostic ultrasound: principles and instruments*: WB Saunders, 1998.

[2] J. A. Hossack, T. S. Sumanaweera, S. Napel, and J. S. Ha, "Quantitative 3-D diagnostic ultrasound imaging using a modified transducer array and an automated image tracking technique," *Ultrasonics, Ferroelectrics and Frequency Control, IEEE Transactions on,* vol. 49, pp. 1029-1038, 2002.

[3] D. Gobbi, R. Comeau, and T. Peters, "Ultrasound probe tracking for real-time ultrasound/MRI overlay and visualization of brain shift," in *Medical Image Computing and Computer-Assisted Intervention*, 1999, pp. 920-927.

[4] Y. Yu and S. T. Acton, "Speckle reducing anisotropic diffusion," *Image Processing, IEEE Transactions on,* vol. 11, pp. 1260-1270, 2002.

[5] P. C. Tay, C. D. Garson, S. T. Acton, and J. A. Hossack, "Ultrasound despeckling for contrast enhancement," *Image Processing, IEEE Transactions on,* vol. 19, pp. 1847-1860, 2010.

[6] R. Rubinstein, M. Zibulevsky, and M. Elad, "Double sparsity: Learning sparse dictionaries for sparse signal approximation," *Signal Processing, IEEE Transactions on,* vol. 58, pp. 1553-1564, 2010.

[7] J. Kwon, S. Cho, Y. Ahn, and Y. Ro, "Noise reduction in DEXA image based on system noise modeling," in *Biomedical and Pharmaceutical Engineering, International Conference on*, 2009, pp. 1-6.

[8] M. Elad and M. Aharon, "Image denoising via sparse and redundant representations over learned dictionaries," *Image Processing, IEEE Transactions on,* vol. 15, pp. 3736-3745, 2006.

[9] J. Wright, A. Y. Yang, A. Ganesh, S. S. Sastry, and Y. Ma, "Robust face recognition via sparse representation," *Pattern Analysis and Machine Intelligence, IEEE Transactions on,* vol. 31, pp. 210-227, 2009.

[10] R. Rubinstein, M. Zibulevsky, and M. Elad, "Efficient implementation of the K-SVD algorithm using batch orthogonal matching pursuit," *CS Technion,* 2008.

[11] A. B. Watson, "Image compression using the discrete cosine transform," *Mathematica journal,* vol. 4, p. 81, 1994.

[12] M. Aharon, M. Elad, and A. Bruckstein, "K-SVD: An Algorithm for Designing Overcomplete Dictionaries for Sparse Representation," *Signal Processing, IEEE Transactions on,* vol. 54, pp. 4311-4322, 2006.

[13] X. Zong, A. F. Laine, and E. A. Geiser, "Speckle reduction and contrast enhancement of echocardiograms via multiscale nonlinear processing," *Medical Imaging, IEEE Transactions on,* vol. 17, pp. 532-540, 1998.

[14] A. Achim, A. Bezerianos, and P. Tsakalides, "Novel Bayesian multiscale method for speckle removal in medical ultrasound images," *Medical Imaging, IEEE Transactions on,* vol. 20, pp. 772-783, 2001.

[15] J. Bamber and R. Dickinson, "Ultrasonic B-scanning: a computer simulation," *Physics in medicine and biology,* vol. 25, p. 463, 2000.

[16] C. Butakoff, S. Balocco, S. Ordas, and A. F. Frangi, "Simulated 3D ultrasound LV cardiac images for active shape model training," in *SPIE Medical Imaging*, 2007.

[17] Z. Wang, A. C. Bovik, H. R. Sheikh, and E. P. Simoncelli, "Image quality assessment: From error visibility to structural similarity," *Image Processing, IEEE Transactions on,* vol. 13, pp. 600-612, 2004.

[18] F. Sattar, L. Floreby, G. Salomonsson, and B. Lovstrom, "Image enhancement based on a nonlinear multiscale method," *Image Processing, IEEE Transactions on,* vol. 6, pp. 888-895, 1997.